

# Photo-physiological variability in phytoplankton chlorophyll fluorescence and assessment of chlorophyll concentration

Alexander Chekalyuk\* and Mark Hafez

Lamont Doherty Earth Observatory of Columbia University, 61 Route 9W, Palisades, New York 10964, USA

\*[chekaluk@ldeo.columbia.edu](mailto:chekaluk@ldeo.columbia.edu)

**Abstract:** Photo-physiological variability of *in vivo* chlorophyll fluorescence (*CF*) per unit of chlorophyll concentration (*CC*) is analyzed using a biophysical model to improve the accuracy of *CC* assessments. Field measurements of *CF* and photosystem II (PSII) photochemical yield (*PY*) with the Advanced Laser Fluorometer (ALF) in the Delaware and Chesapeake Bays are analyzed vs. high-performance liquid chromatography (HPLC) *CC* retrievals. It is shown that isolation from ambient light, PSII saturating excitation, optimized phytoplankton exposure to excitation, and phytoplankton dark adaptation may provide accurate *in vivo* *CC* fluorescence measurements ( $R^2 = 0.90\text{--}0.95$  vs. HPLC retrievals). For *in situ* or flow-through measurements that do not allow for dark adaptation, concurrent *PY* measurements can be used to adjust for *CF* non-photochemical quenching (*NPQ*) and improve the accuracy of *CC* fluorescence assessments. Field evaluation has shown the *NPQ*-invariance of *CF/PY* and *CF(PY<sup>-1</sup>-1)* parameters and their high correlation with HPLC *CC* retrievals ( $R^2 = 0.74\text{--}0.96$ ), while the *NPQ*-affected *CF* measurements correlated poorly with *CC* ( $R^2 = -0.22$ ).

©2011 Optical Society of America

**OCIS codes:** (010.4450) Oceanic optics; (280.4788) Optical sensing and sensors; (300.0300) Spectroscopy; (140.0140) Lasers and laser optics.

---

## References and links

1. G. C. Papageorgiou and Govindjee (Eds.), *Chlorophyll a Fluorescence: A Signature of Photosynthesis*, *Advances in Photosynthesis and Respiration* (Springer, Dordrecht, 2004).
2. T. J. Cowles, J. N. Moum, R. A. Desiderio, and S. M. Angel, "In situ monitoring of ocean chlorophyll via laser-induced fluorescence backscattering through an optical fiber," *Appl. Opt.* **28**(3), 595–600 (1989).
3. E. J. D'Sa, S. E. Lohrenz, J. H. Churchill, V. L. Asper, J. L. Largier, and A. J. Williams III, "Chlorophyll distribution and transport on the inner shelf off Duck, North Carolina," *J. Geophys. Res.- Oceans* **106**(C6), 11581–11596 (2001).
4. C. E. Del Castillo, P. G. Coble, R. N. Conmy, F. E. Muller-Karger, L. Vanderbloemen, and G. A. Vargo, "Multispectral in situ measurements of organic matter and chlorophyll fluorescence in seawater: Documenting the intrusion of the Mississippi River plume in the West Florida Shelf," *Limnol. Oceanogr.* **46**(7), 1836–1843 (2001).
5. Z. Kolber and P. G. Falkowski, "Use of active fluorescence to estimate phytoplankton photosynthesis in-situ," *Limnol. Oceanogr.* **38**(8), 1646–1665 (1993).
6. M. J. Perry, B. S. Sackmann, C. C. Eriksen, and C. M. Lee, "Seaglider observations of blooms and subsurface chlorophyll maxima off the Washington coast," *Limnol. Oceanogr.* **53**(5\_part\_2), 2169–2179 (2008).
7. S. Babichenko, S. Kaitala, A. Leeben, L. Poryvkina, and J. Seppala, "Phytoplankton pigments and dissolved organic matter distribution in the Gulf of Riga," *J. Mar. Syst.* **23**(1-3), 69–82 (1999).
8. A. M. Chekalyuk, F. E. Hoge, C. W. Wright, R. N. Swift, and J. K. Yungel, "Airborne test of laser pump-and-probe technique for assessment of phytoplankton photochemical characteristics," *Photosynth. Res.* **66**(1/2), 45–56 (2000).
9. J. H. Churnside and P. L. Donaghay, "Thin scattering layers observed by airborne lidar," *ICES J. Mar. Sci.* **66**(4), 778–789 (2009).

10. F. E. Hoge and R. N. Swift, "Airborne simultaneous spectroscopic detection of laser-induced water Raman backscatter and fluorescence from chlorophyll a and other naturally occurring pigments," *Appl. Opt.* **20**(18), 3197–3205 (1981).
11. M. Beutler, K. H. Wiltshire, B. Meyer, C. Moldaenke, C. Lüring, M. Meyerhöfer, U. P. Hansen, and H. Dau, "A fluorometric method for the differentiation of algal populations *in vivo* and *in situ*," *Photosynth. Res.* **72**(1), 39–53 (2002).
12. A. Chekalyuk and M. Hafez, "Advanced laser fluorometry of natural aquatic environments," *Limnol. Oceanogr. Methods* **6**, 591–609 (2008).
13. T. J. Cowles, R. A. Desiderio, and S. Neuer, "In situ characterization of phytoplankton from vertical profiles of fluorescence emission-spectra," *Mar. Biol.* **115**(2), 217–222 (1993).
14. G. Parésys, C. Rigart, B. Rousseau, A. W. M. Wong, F. Fan, J. P. Barbier, and J. Lavaud, "Quantitative and qualitative evaluation of phytoplankton communities by trichromatic chlorophyll fluorescence excitation with special focus on cyanobacteria," *Water Res.* **39**(5), 911–921 (2005).
15. C. W. Proctor and C. S. Roesler, "New insights on obtaining phytoplankton concentration and composition from *in situ* multispectral chlorophyll fluorescence," *Limnol. Oceanogr. Methods* **8**, 695–708 (2010).
16. T. L. Richardson, E. Lawrenz, J. L. Pinckney, R. C. Guajardo, E. A. Walker, H. W. Paerl, and H. L. MacIntyre, "Spectral fluorometric characterization of phytoplankton community composition using the Algae Online Analyser," *Water Res.* **44**(8), 2461–2472 (2010).
17. T. S. Bibby, M. Y. Gorbunov, K. W. Wyman, and P. G. Falkowski, "Photosynthetic community responses to upwelling in mesoscale eddies in the subtropical North Atlantic and Pacific Oceans," *Deep Sea Res. Part II Top. Stud. Oceanogr.* **55**(10-13), 1310–1320 (2008).
18. A. M. Chekalyuk, F. E. Hoge, C. W. Wright, and R. N. Swift, "Short-pulse pump-and-probe technique for airborne laser assessment of Photosystem II photochemical characteristics," *Photosynth. Res.* **66**(1/2), 33–44 (2000).
19. P. Falkowski and D. A. Kiefer, "Chlorophyll-a fluorescence in phytoplankton - relationship to photosynthesis and biomass," *J. Plankton Res.* **7**(5), 715–731 (1985).
20. P. G. Falkowski and Z. Kolber, "Variations in chlorophyll fluorescence yields in phytoplankton in the world oceans," *Aust. J. Plant Physiol.* **22**(2), 341–355 (1995).
21. T. Fujiki, T. Hosaka, H. Kimoto, T. Ishimaru, and T. Saino, "In situ observation of phytoplankton productivity by an underwater profiling buoy system: use of fast repetition rate fluorometry," *Mar. Ecol. Prog. Ser.* **353**, 81–88 (2008).
22. M. Y. Gorbunov, P. G. Falkowski, and Z. S. Kolber, "Measurement of photosynthetic parameters in benthic organisms *in situ* using a SCUBA-based fast repetition rate fluorometer," *Limnol. Oceanogr.* **45**(1), 242–245 (2000).
23. Z. Kolber, K. D. Wyman, and P. G. Falkowski, "Natural variability in photosynthetic energy-conversion efficiency - a field-study in the Gulf of Maine," *Limnol. Oceanogr.* **35**(1), 72–79 (1990).
24. Z. Kolber and P. G. Falkowski, "Use of active fluorescence to estimate phytoplankton photosynthesis *in-situ*," *Limnol. Oceanogr.* **38**(8), 1646–1665 (1993).
25. R. J. Olson, A. M. Chekalyuk, and H. M. Sosik, "Phytoplankton photosynthetic characteristics from fluorescence induction assays of individual cells," *Limnol. Oceanogr.* **41**(6), 1253–1263 (1996).
26. R. J. Olson, H. M. Sosik, and A. M. Chekalyuk, "Photosynthetic characteristics of marine phytoplankton from pump-during-probe fluorometry of individual cells at sea," *Cytometry* **37**(1), 1–13 (1999).
27. R. J. Olson, H. M. Sosik, A. M. Chekalyuk, and A. Shalapyonok, "Effects of iron enrichment on phytoplankton in the Southern Ocean during late summer: active fluorescence and flow cytometric analyses," *Deep Sea Res. Part II Top. Stud. Oceanogr.* **47**(15-16), 3181–3200 (2000).
28. M. P. Raateoja, "Fast repetition rate fluorometry (FRRF) measuring phytoplankton productivity: a case study at the entrance to the Gulf of Finland, Baltic Sea," *Boreal Environ. Res.* **9**, 263–276 (2004).
29. Y. Huot, M. Babin, F. Bruyant, C. Grob, M. S. Twardowski, and H. Claustre, "Relationship between photosynthetic parameters and different proxies of phytoplankton biomass in the subtropical ocean," *Biogeosciences* **4**(5), 853–868 (2007).
30. M. Kruskopf and K. J. Flynn, "Chlorophyll content and fluorescence responses cannot be used to gauge reliably phytoplankton biomass, nutrient status or growth rate," *New Phytol.* **169**(3), 525–536 (2006).
31. O. C. Swertz, F. Colijn, H. W. Hofstraat, and B. A. Althuis, "Temperature, salinity, and fluorescence in Southern North Sea: high-resolution data sampled from a ferry," *Environ. Manage.* **23**(4), 527–538 (1999).
32. C. D. Wirick, "Exchange of phytoplankton across the continental shelf-slope boundary of the Middle Atlantic Bight during spring-1988," *Deep Sea Res. Part II Top. Stud. Oceanogr.* **41**(2-3), 391–410 (1994).
33. A. E. Alpine and J. E. Cloern, "Differences in *in vivo* fluorescence yield between three phytoplankton size classes," *J. Plankton Res.* **7**(3), 381–390 (1985).
34. J. J. Cullen, "The deep chlorophyll maximum - comparing vertical profiles of chlorophyll-a," *Can. J. Fish. Aquat. Sci.* **39**(5), 791–803 (1982).
35. J. J. Cullen and M. R. Lewis, "Biological processes and optical measurements near the sea surface: Some issues relevant to remote sensing," *J. Geophys. Res. - Oceans* **100**(C7), 13255–13266 (1995).
36. M. E. Loftus and H. H. Seliger, "Some limitations of the *in vivo* fluorescence technique," *Chesap. Sci.* **16**(2), 79–92 (1975).

37. T. Jakob, U. Schreiber, V. Kirchesch, U. Langner, and C. Wilhelm, "Estimation of chlorophyll content and daily primary production of the major algal groups by means of multiwavelength-excitation PAM chlorophyll fluorometry: performance and methodological limits," *Photosynth. Res.* **83**(3), 343–361 (2005).
38. Z. S. Kolber, O. Prasil, and P. G. Falkowski, "Measurements of variable chlorophyll fluorescence using fast repetition rate techniques: defining methodology and experimental protocols," *BBA.- Bioenergetics* **1367**(1-3), 88–106 (1998).
39. G. H. Krause and E. Weis, "Chlorophyll fluorescence and photosynthesis - the basics," *Annu. Rev. Plant Physiol.* **42**(1), 313–349 (1991).
40. T. R. Jacobsen, "A quantitative method for the separation of chlorophyll a and b from phytoplankton pigments by HPLC," *Mar. Sci. Comm.* **4**, 33–47 (1978).
41. C. J. Lorenzen, "Determination of chlorophyll and phaeo-pigments - spectrophotometric equations," *Limnol. Oceanogr.* **12**(2), 343–346 (1967).
42. O. C. J. Holm-Hansen, C. J. Lorenzen, R. W. Holmes, and J. D. H. Strickland, "Fluorometric determination of chlorophyll," *J. Cons. Perm. Int. Explor. Mer.* **30**, 3–15 (1965).
43. Govindje, "63 years since Kautsky - chlorophyll-a fluorescence," *Aust. J. Plant Physiol.* **22**(2), 131–160 (1995).
44. G. C. Papageorgiou, M. Tsimilli-Michael, and K. Stamatakis, "The fast and slow kinetics of chlorophyll a fluorescence induction in plants, algae and cyanobacteria: a viewpoint," *Photosynth. Res.* **94**(2-3), 275–290 (2007).
45. J. C. Kromkamp and R. M. Forster, "The use of variable fluorescence measurements in aquatic ecosystems: differences between multiple and single turnover measuring protocols and suggested terminology," *Eur. J. Phycol.* **38**(2), 103–112 (2003).
46. S. I. Heaney, "Some observations on use of *in vivo* fluorescence technique to determine chlorophyll-a in natural-populations and cultures of freshwater phytoplankton," *Freshw. Biol.* **8**(2), 115–126 (1978).
47. A. Stirbet and Govindjee, "On the relation between the Kautsky effect (chlorophyll a fluorescence induction) and Photosystem II: basic and applications of the OJIP fluorescence transient," *J. Photochem. Photobiol. B* **104**(1-2), 236–257 (2011).
48. S. T. Sweet and N. L. Guinasso, "Effects of flow-rate on fluorescence *in vivo* during continuous measurements on Gulf of Mexico surface-water," *Limnol. Oceanogr.* **29**(2), 397–401 (1984).
49. R. Röttgers, "Comparison of different variable chlorophyll a fluorescence techniques to determine photosynthetic parameters of natural phytoplankton," *Deep Sea Res. Part I Oceanogr. Res. Pap.* **54**(3), 437–451 (2007).
50. A. M. Chekalyuk, Lamont Doherty Earth Observatory of Columbia University, 61 Route 9W, Palisades, NY 10964, M. Landry, R. Goericke, A. G. Taylor, and M. Hafez are preparing a manuscript to be called "Laser fluorescence phytoplankton analysis across a frontal zone in the California Current Ecosystem."

## 1. Introduction

Chlorophyll *a* (Chl) is a photosynthetic pigment that plays a key role in photosynthesis [1]. All phytoplankton species, regardless of their specific group and taxonomic features, contain Chl in their photosynthetic apparatus. Chl concentration (*CC*) is broadly used as a useful index of phytoplankton biomass in laboratory research, oceanographic studies, and environmental surveys. *In vivo* measurements of Chl fluorescence (*CF*) are highly sensitive, fast and easy to conduct in a small sample volume at natural concentrations of the photosynthesizing microorganisms, including direct *in situ* measurements [2–6] and LIDAR remote sensing [7–10]. *CF* measurements can provide information about *CC*, phytoplankton community structure [11–16], physiological status, photosynthetic efficiency and productivity [17–28].

While *CF* is broadly used as a proxy of *CC* and phytoplankton biomass [19, 29–32], the accuracy of quantitative *CC* assessments is often compromised by high, up to an order of magnitude [33–36], variability in *CF/CC* ratio. The relationship between *CF* and *CC* depends on phytoplankton taxonomy, cell size, organization of photosynthetic apparatus and physiological status. Even frequent instrument calibrations cannot guarantee reliable and accurate *CC* fluorescence retrievals. *CF* photo-physiological regulation by light regime and nutrient availability is known to be one of the major factors affecting *CF/CC* variability (e.g [19, 35]). The appropriate choice of a measurement protocol may result in the *CF/CC* variability reduction. Some fluorometers [12, 17, 21, 22, 37, 38] provide measurements of physiological parameters that potentially can be used to adjust *CF* magnitudes affected by photo-physiological variability.

In this article, we use a simplified biophysical model to illustrate the problems relevant to the *CF* photo-physiological regulation and provide some practical recommendations that may

help to improve the accuracy of *CC* assessment from *in vivo CF* measurements. The analytical results and measurement protocols are evaluated using field measurements in the Delaware and Chesapeake Bays. The abbreviations and variables used in the article are listed in Table 1.

**Table 1. Abbreviations and Variables**

Abbreviation or variable	Meaning
Chl	Chlorophyll
CC	Chl concentration, $\text{mg m}^{-3}$
CF or CF'	Chl fluorescence measured in a dark- or light-adapted state of phytoplankton, respectively (subscripts "U" and "S" designate flow-through underway and sample measurements, respectively)
CFY	Chl fluorescence yield
HPLC	High-performance liquid chromatography
PSII	Photosystem II
RCs	Reaction centers
PQ	Photochemical quenching
NPQ	Non-photochemical quenching
ALF	Advanced Laser Fluorometer
ST	PSII single-turnover time scale, $< 1$ ms
MT	PSII multi-turnover time scale, $> 1$ ms
f	Fraction of the photochemically functional PSII reaction centers; $0 < f < 1$
A	Fraction of open functional PSII reaction centers; $0 < A < 1$
$k_p$	Rate constant of PSII photochemistry
$k_f$	Rate constant of PSII Chl fluorescence
$k_d$	Rate constant of PSII constitutive heat dissipation
$k_N$	Rate constant of NPQ heat dissipation
$\Phi_p$ or $\Phi_p'$	PSII photochemical yield in a dark- or light-adapted state of phytoplankton, respectively
$\Phi_p^m$ or $\Phi_p^{m'}$	Maximal PSII photochemical yield in a dark- or light-adapted state of phytoplankton, respectively
$\Phi_f$ or $\Phi_f'$	PSII CFY in a dark- or light-adapted states of phytoplankton, respectively
$\Phi_o$ or $\Phi_o'$	Minimum PSII CFY in a dark- or light-adapted states of phytoplankton, respectively
$\Phi_m$ or $\Phi_m'$	Maximum PSII CFY in a dark- or light-adapted states of phytoplankton, respectively. Subscripts (ST) or (MT) designate measurements at PSII single- or multi-turnover time scale, respectively
PY	Maximal potential PSII photochemical yield in a dark- or light-adapted state of phytoplankton measured at ST time scale
V	water volume that contains phytoplankton, $\text{m}^3$
$\sigma$	Chl absorption cross-section, $\text{m}^2$
I	fluorescence excitation intensity, $\text{photons m}^{-2} \text{s}^{-1}$
$n_{\text{PSII}}$	fraction of Chl molecules associated with PSII

## 2. Photo-physiological regulation of chlorophyll fluorescence (model analysis)

Chl molecules are incorporated in phytoplankton cells and, therefore, are not evenly distributed in the water. Nonetheless, *CC* is commonly accepted for estimating the average Chl biomass per unit of water volume containing phytoplankton. Most *in vivo CF* originates from the Chl molecules of the light-harvesting antenna of photosystem II (PSII) in the photosynthetic apparatus of phytoplankton [39]. The relationship between *CF* intensity and *CC* can be described as

$$CF = K * CC = N_A M^{-1} V \sigma I \Phi_f n_{\text{PSII}} CC = k \Phi_f * CC. \quad (1)$$

Here, *V* is the water volume containing phytoplankton and exposed to fluorescence excitation,  $\sigma$  is the absorption cross-section of Chl molecules, *I* is the excitation intensity,  $\Phi_f$  is the PSII *CF* yield (*CFY*),  $n_{\text{PSII}}$  is the fraction of Chl molecules associated with PSII,  $N_A$  is the Avogadro constant, and *M* is Chl molar mass. The conventional approach to *in vivo CC* fluorescence measurements is determining the parameter  $K = N_A M^{-1} V \sigma I \Phi_f n_{\text{PSII}}$  via fluorometer calibration and using it for conversion of the *CF* measurements into the *CC* units:

$CC = K^{-1}CF$ . The calibration involves the measurements of  $CF$  (with the fluorometer to be calibrated) and  $CC$  (using one of the independent analytical techniques) in phytoplankton-containing water samples, and regression analysis of  $CF$  vs.  $CC$ . HPLC [40], spectrophotometric [41], or fluorometric [42] methods can be used for  $CC$  measurements. A similar approach works well for measuring concentration of dissolved fluorescent organic molecules, but the accuracy of  $CC$  assessments from *in vivo*  $CF$  measurements is often compromised. There are various structural and physiological factors and regulatory mechanisms in phytoplankton that may affect the biological variables  $n_{\text{PSII}}$ ,  $\sigma$ , and  $\Phi_f$  in Eq. (1) and, respectively, the  $CF/CC$  ratio, making applicability of even frequent field calibrations problematic. A detailed discussion on this topic is beyond the scope of this article; some relevant information can be found in [1, 19, 20, 35]. Below we use a simplified biophysical model (following [19, 20, 39, 43]) to analyze the most relevant aspects of the  $CFY$  photo-physiological variability as one of the major factors affecting the  $CF/CC$  ratio.

The PSII  $CF$  and thermal dissipation represent two channels of energy losses accompanying the PSII photochemical reactions. The quantum yields of photochemistry and fluorescence for dark-adapted PSII can be described, respectively, as:

$$\Phi_p = fAk_p / (Afk_p + k_f + k_d) \quad (2)$$

$$\Phi_f = k_f / (Afk_p + k_f + k_d). \quad (3)$$

Here,  $k_p$ ,  $k_f$ , and  $k_d$  are, respectively, the rate constants of photochemistry in functional PSII reaction centers (RCs), fluorescence and constitutive heat dissipation. The parameter  $f$  represents the fraction of the photochemically functional PSII reaction centers (RCs) ( $0 < f < 1$ );  $A$  represents the fraction of the open functional PSII RCs ( $0 < A < 1$ ). The dependence of  $\Phi_p$  and  $\Phi_f$  on these photochemical parameters is described in terms of photochemical quenching ( $PQ$ ). The magnitude of  $f$  mainly depends on the nutrient supply and light conditions, while  $A$  is determined by the dynamic equilibrium between photochemical closing and re-opening of PSII RCs (e.g., [25]). In particular, when  $A = 0$  (all PSII RCs are closed under the intense, PSII saturating incident light),  $\Phi_f$  reaches its maximal magnitude,  $\Phi_m$ :

$$\Phi_m = k_f / (k_f + k_d). \quad (4)$$

When  $A = 1$  (all PSII RCs are open in darkness),  $\Phi_f$  reaches its minimal magnitude:

$$\Phi_o = k_f / (fk_p + k_f + k_d). \quad (5)$$

In darkness ( $A = 1$ ) the  $\Phi_p$  maximal potential magnitude can be expressed via  $\Phi_o$  and  $\Phi_m$  as

$$\Phi_p^m = fk_p / (fk_p + k_f + k_d) = (\Phi_m - \Phi_o) / \Phi_m \quad (6)$$

The  $\Phi_o/\Phi_m$  ratio can be calculated from Eq. (6) as

$$\Phi_o / \Phi_m = 1 - \Phi_p^m. \quad (7)$$

An exposure to excessive ambient light may result in the gradual development of non-photochemical quenching ( $NPQ$ ) that enhances thermal dissipation of the absorbed light energy. There are several photo-protective  $NPQ$  mechanisms (e.g., [39]). Depending on the intensity of incident light and the  $NPQ$  mechanisms involved,  $NPQ$  may develop over time scales ranging from seconds to minutes [44]. Recovery from  $NPQ$  action in dark conditions may require several minutes to several hours.  $NPQ$  can be described with an additional  $NPQ$  rate constant,  $k_N$  [39]. The actual maximal and minimal  $CFY$  magnitudes, and the maximal potential quantum yield of PSII photochemistry for the  $NPQ$ -affected photosystem can be expressed, respectively, as

$$\Phi'_p = fAk_p / (Afk_p + k_f + k_d + k_N) \quad (8)$$

$$\Phi'_f = k_f / (Afk_p + k_f + k_d + k_N) \quad (9)$$

$$\Phi'_m = k_f / (k_f + k_d + k_N) \quad (10)$$

$$\Phi'_o = k_f / (fk_p + k_f + k_d + k_N) \quad (11)$$

$$\Phi'_p{}^m = fk_p / (fk_p + k_f + k_d + k_N) = (\Phi'_m - \Phi'_o) / \Phi'_m. \quad (12)$$

From Eqs. (4), (10):

$$\Phi_m / \Phi'_m = 1 + k_N / (k_f + k_d) = 1 + NPQ. \quad (13)$$

From Eqs. (5), (6), (11), and (12):

$$\Phi_o / \Phi'_o = \Phi_p{}^m / \Phi'_p{}^m = 1 + k_N / (fk_p + k_f + k_d) = 1 + (fk_p / k_N + NPQ^{-1})^{-1} \quad (14)$$

$$\Phi_f / \Phi'_f = \Phi_p / \Phi'_p = 1 + k_N / (Afk_p + k_f + k_d) = 1 + (Afk_p / k_N + NPQ^{-1})^{-1}. \quad (15)$$

Here,  $NPQ = k_N / (k_f + k_d)$ , a parameter that is often used for quantitative  $NPQ$  assessment [45]. Using Eqs. (13)-(15), the relative  $NPQ$ -induced changes in the fluorescence and photochemical yields can be estimated as

$$(\Phi_f - \Phi'_f) / \Phi'_f = (\Phi_p - \Phi'_p) / \Phi'_p = (Afk_p / k_N + NPQ^{-1})^{-1} \quad (16)$$

$$(\Phi_o - \Phi'_o) / \Phi'_o = (\Phi_p{}^m - \Phi'_p{}^m) / \Phi'_p{}^m = (fk_p / k_N + NPQ^{-1})^{-1} \quad (17)$$

$$(\Phi_m - \Phi'_m) / \Phi'_m = NPQ. \quad (18)$$

Thus,  $NPQ$  development should cause the most pronounced decrease in  $\Phi'_m$ . Declines in  $\Phi'_o$  and  $\Phi'_p{}^m$  induced by  $NPQ$  are smaller and dependent on the phytoplankton physiological status (described by  $f$  in the model).

From Eqs. (7), (14), and (15) it follows that

$$\Phi_f / \Phi_p = \Phi'_f / \Phi'_p, \text{ and} \quad (19)$$

$$\Phi_m (1 / \Phi_p{}^m - 1) = \Phi'_m (1 / \Phi'_p{}^m - 1). \quad (20)$$

### 3. Recommendations on CF measurement protocol for improved CC assessments

Thus, the phytoplankton  $CFY$  generally depends on the PSII photochemical functionality and the actual intensity of the incident light (both determine the  $PQ$ ), as well as on the phytoplankton light exposure prior to the measurements that determine the  $NPQ$ . A potential range of the  $CFY$  photo-physiological variability can be estimated using the above analysis. The maximum value of  $\Phi_p{}^m \sim 0.65$  measured in healthy phytoplankton [5, 20] would result in  $\Phi_m / \Phi_o \sim 3$  (Eq. (6)). Thus, the  $\Phi_f$  magnitude can vary up to 3-fold, depending on the actual  $PQ$  effect (Eq. (2)). Our field data show that up to a 5-fold  $NPQ$ -induced  $CFY$  decline can be observed in the subsurface water column around noon (e.g., Fig. 3A), depending on the light conditions and mixing regime. The maximum range of  $CFY$  natural variability caused by both  $PQ$  and  $NPQ$  can be estimated then as 15. This estimate is markedly close to the  $\sim 12$ -fold  $CF/CC$  variability observed in the field (e.g., [46]), suggesting that the  $CFY$  photo-

physiological regulation may be one of the major factors affecting the overall variability in the relationship between *CF* and *CC*.

During the active *CF* measurements, the *PQ* and *NPQ* magnitudes may depend on both ambient and *CF* excitation light. *CF* efficiency can vary a great deal, depending on environmental conditions, measurement protocols and phytoplankton physiological status. This provides unique opportunities for fluorescence assessment of phytoplankton photo-physiological characteristics (e.g., [25, 38]). On the other hand, *CFY* variability needs to be minimized or accounted for to improve the accuracy of *CC* fluorescence assessments.

Phytoplankton exposure to ambient light activates a complex chain of photosynthetic reactions and photo-adaptive physiological transformations and may result in *NPQ* development that significantly affects the *CFY* magnitude [39, 44, 47]. If measurement conditions permit, keeping water samples in low-light conditions for at least one hour before the measurement may restore the dark-adapted  $\Phi_o$  level of *CFY*, which is independent of the prior “light history” of phytoplankton. It should be noted that after phytoplankton exposure to intense irradiance, even several hours of dark adaptation may be insufficient for complete recovery from *NPQ* [44] (for example, see Fig. 3B and Discussion).

Optical isolation of the measured sample volume eliminates the *PQ* component associated with the ambient light thus minimizing the overall *CFY* variability. If ambient light is blocked, *PQ* is determined by the intensity of excitation light and depends on PSII photochemical functionality (determined by *f* in the model). The *PQ* component and *CFY* dependence on the PSII physiology can be further minimized by using the PSII saturating fluorescence excitation that dynamically closes the PSII RCs to reach the  $CFY \sim \Phi_m$  at the beginning of the fluorescence measurement. This also eliminates the need for optical isolation of the measured sample volume ( $PQ \sim 0$  regardless of the ambient light), which may simplify the *in situ* *CF* measurements.

The physiological origin of *in vivo* *CF* results in a complex *CFY* time transient after initiating the excitation known as Kautsky effect (e.g [44, 47]). It includes a polyphasic rise from the initial  $\Phi_o$  level to its maximum  $\Phi_m$  value ( $\Phi'_o$  and  $\Phi'_m$ , respectively, for light-adapted phytoplankton) followed by a polyphasic decline to some stationary *CFY* magnitude. The induction rise begins with a fast, photochemical phase (< 1 ms) followed by several thermal phases to reach  $\Phi_m$  in ~100 ms under intense PSII saturating excitation [44, 47]. *CFY* remains almost unchanged at the maximum level for several seconds and gradually declines after that over 0.1 – 1 minute due to the development of excitation-induced *NPQ*.

Thus, *CFY* may continuously vary during the *in vivo* *CF* measurement due to the physiological mechanisms involved in the Kautsky effect, and the integral *CF* value is usually determined by the average *CFY* magnitude over the measurement time (this is discussed below regarding the ALF *CF* measurements). Several instrumental factors (e.g., excitation intensity and duration, measurement time, sample exposure to the excitation, etc.) may affect the average *CFY* value and result in a variable, instrument and protocol dependent *CF/CC* relationship. For example, the *CF* magnitude may appear to be dependent on the sample flow rate through the measurement chamber (e.g., [48]).

If a PSII saturating excitation is used for minimizing the *PQ* component of the *CFY* variability, it may be beneficial to limit the sample exposure to the excitation to ~1 second. Then the *CF* measurement will be conducted for most of the measurement time at the maximum level of *CFY*, independent of PSII photochemical functionality and not affected by the excitation-induced *NPQ* that would develop at the longer sample exposure. The actual measurement time may be longer if the measurements are conducted in a fast enough sample flow to limit the exposure time of the measured sample volume.

To summarize, the effect of *CFY* photo-physiological variability on the *CF* measurements can be reduced by the following (referred below as a “four-step measurement protocol”):

1. Isolating measurement volume from ambient light to reduce its effect on the *CFY* variability.
2. Using PSII saturating fluorescence excitation to minimize the *CFY* dependence on PSII photochemical functionality.
3. Optimizing sample exposure to the excitation to minimize the *CFY* variability (~1 second exposure may be optimal for the PSII saturating excitation).
4. Providing phytoplankton dark adaptation before the measurements (if conditions permit).

It is technically difficult to provide phytoplankton dark adaptation when conducting daytime *in situ* or flow-through underway shipboard measurements. The *CF* intensity may be *NPQ*-affected due to phytoplankton exposure to the ambient light in the water column. The *NPQ* effect may depend on the unknown phytoplankton “light history” and compromise the accuracy of *CC* fluorescence retrievals. The above model analysis shows that the PSII photochemical yield also exhibits the *NPQ* down-regulation (Eqs. (14), (15)). Therefore, the concurrent *PY* measurements may provide a potential way to adjust the *CF* retrievals for the *NPQ* effect. Equations (19) and (20) illustrate this idea, showing that the fluorescence parameters  $\Phi_f/\Phi_p$  and  $\Phi_m(1/\Phi_p^m - 1)$  should remain invariant regardless of the *NPQ* magnitude and equal to their values in the PSII dark-adapted state. There are various measurement protocols and instruments for *PY* assessments [12, 37, 38, 49], so the practical implementations of this approach needs evaluation and optimization on a case-by-case basis. Below, we demonstrate with field data that the *CF NPQ*-adjustment using the *PY* measurements may provide a significant advantage over the conventional, *CF*-based *CC* assessments when it is problematic to provide phytoplankton recovery from the *NPQ* (e.g., *in situ* and flow-through underway retrievals). On the other hand, a potential dependence of the *NPQ*-invariant parameters on various physiological mechanisms needs to be evaluated (see Discussion).

#### 4. Field measurements with advanced laser fluorometer

The field measurements with the Advanced Laser Fluorometer (ALF) were used to evaluate our analytical conclusions and proposed measurement protocols for improving the accuracy of *CC* fluorescence assessments. ALF is a compact field instrument that provides both spectrally and temporally resolved fluorescence measurements. Its design and measurement protocols are described in detail in [12]. The ALF conducts spectral deconvolution of the laser-stimulated emission to provide measurements of Chl, phycoerythrin, and CDOM fluorescence. The fluorescence intensities are normalized to water Raman scattering to account for variability in water optical properties. The ALF measurements of variable fluorescence are spectrally corrected for the non-*CF* background to improve the accuracy of retrievals.



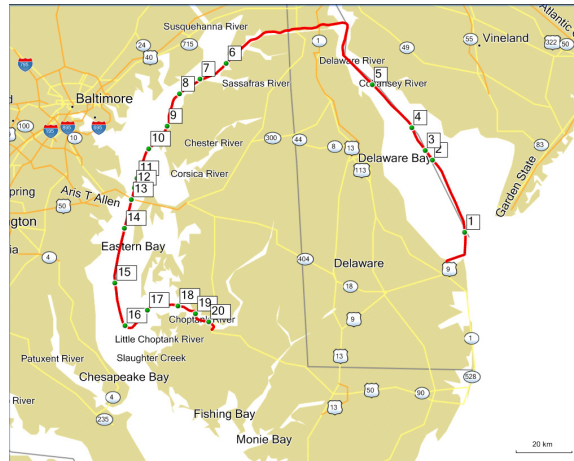


Fig. 1. A map of shipboard ALF underway flow-through measurements in the Delaware and Chesapeake Bays, April 15–16 2008. Green dots display the sampling locations for laboratory measurements of Chl fluorescence and concentration.

The following features of the ALF design and measurement protocols make this instrument suitable for the field test of the above analytical conclusions. The ALF measurement cell is located in the sample compartment inside the instrument case and isolated from ambient light (condition 1 in Section 3). The spot size of the 405 nm laser excitation beam used for *CF* and *VF* measurements is appropriately adjusted to saturate PSII over  $\sim 100 \mu\text{s}$  (condition 2 in Section 3), thus providing the *PY* retrievals at PSII single-turnover (ST) time scale (e.g., [25, 45]). The spectral integration time with 405 nm excitation is limited to 1 second to avoid development of the laser-stimulated *NPQ* that happens over longer time scales (condition 3 in Section 3). About one hour of dark adaptation is provided for discrete water samples before *in vivo* fluorescence measurements with the ALF instrument (condition 4 in Section 3).

The results reported in this article are essentially based on comparison of the *CF* and *PY* measurements in the dark- and light-adapted states of phytoplankton photosynthetic apparatus. The ALF *CF* field measurements compliant with conditions 1–4 of the above measurement protocol are compared below with the independent HPLC *CC* retrievals. The use of PSII saturating excitation for ALF measurements of both *PY* and *CF* suggests the *NPQ*-invariance of parameter  $CF(PY^{-1}-1)$  (see Eq. (20)). The invariance of this and another fluorescence parameter,  $CF/PY$ , which can be formally derived from Eq. (19), are evaluated using the ALF field measurements and discussed below.

Some aspects of the ALF *CF* measurements relevant to optimizing the sample exposure time need to be briefly discussed. The internal instrument pump for discrete sample analysis operates at the flow rate of 0.1 L/min [12]. It results in  $\sim 100$  ms time of phytoplankton exposure to the PSII saturating excitation (i.e. time of residence in the laser beam). This time corresponds to the PSII multiturnover time (MT) scale, and *CFY* exhibits a polyphasic rise typical for the Kautsky effect [44, 47]. The initial, photochemical phase is identical to the ST fluorescence induction used for the ALF *PY* measurements. It lasts  $\sim 100 \mu\text{s}$ , during which the PSII RCs are gradually closed and *CFY* reaches its maximal ST magnitude  $\Phi_{m(ST)}$  [45]. This initial phase is followed by several thermal phases of continued *CFY* rise to reach its maximum MT level  $\Phi_{m(MT)} \sim 1.5\Phi_{m(ST)}$  [45] at the end of 100 ms exposure time (Fig. 1 in [47]). Though the ALF spectrometer integrates the laser-stimulated emission over  $\sim 1$  s, the *CF* magnitude yielded by the ALF measurements in the sample flow reflects some average over the exposure time *CFY* magnitude,  $\Phi_{m(ST)} < CFY < \Phi_{m(MT)}$ .

During the underway measurements described below in Results, the 1 L/min flow rate has resulted in 10 ms phytoplankton exposure time. Since the intense ( $\sim 0.1$  mol photons  $\text{m}^{-2} \text{s}^{-1}$ ) fluorescence excitation is used in the ALF instrument, the  $CFY$  almost reaches  $\Phi_{m(MT)}$  during the 10 ms exposure and the resulting  $CF$  magnitude is only 10% lower than measured in the samples at 0.1 L/min flow rate (see Results and Discussion). Generally, this magnitude is determined by the fluorescence excitation intensity and the sample flow rate. The latter may explain the  $CF$  dependence on the flow rate often observed with field fluorimeters (e.g., [48]).

The underway shipboard measurements with the ALF instrument were conducted in the Delaware and Chesapeake Bays courtesy of the College of Marine Science (University of Delaware) onboard R/V *Hugh R. Sharp* during its non-stop transit from Lewes (Delaware) to Cambridge (Maryland) (see the map in Fig. 1). The water was continuously sampled by the shipboard sampling system at  $\sim 2$  m below the water surface and directed to the ALF instrument through a 15 m silicon tube at the flow rate of 1 L/min. The delay between sampling and measuring the water was  $\sim 30$  seconds.

The ALF measurement cycle included two measurements of spectral emission in 400–800 nm range using 405 and 532 nm laser excitation, respectively, and the temporally resolved measurement of  $CF$  induction over 100  $\mu\text{s}$  in the spectral range of 670–695 nm using the pump-during-probe measurement protocol [12, 25]. The spectral integration time was 1 s, and the laser excitation was turned off before and after the spectral measurements. The fluorescence induction waveforms were averaged over 5 to 10 flashes of laser excitation at 405 nm and 10 Hz repetition rate.

Twenty water samples were collected along the transect from the discharge of the flow-through system in the 500 mL dark-amber glass bottles and stored in a dark cooler filled with ice. The sampling locations are marked with numbers in Fig. 1. The ALF fluorescence measurements of the samples were conducted at Horn Point Laboratory (University of Maryland Center for Environmental Science) courtesy of Dr. Harding in about 1 hour on arrival to Cambridge. The samples were pumped at 0.1 L/min from the sample bottles through the ALF flow measurement cell. Ten sequent spectral measurements of the sample emission stimulated at 405 nm and 532 nm were conducted in the sample flow. In addition, 10 measurements of fluorescence induction, each averaged over 10 excitation shots, were conducted between the spectral measurements. The spectral and fluorescence induction measurements were averaged over the sequent acquisitions. The collected samples were also filtered for HPLC pigment analysis conducted later at the Pigment Analysis Facility of Horn Point Laboratory.

## 5. Results

Figure 2 displays the results of transect measurements shown in Fig. 1. The measurements began at 19:18 May 15, 2008, continued overnight (see the sunrise mark at 06:24) and were finished at 10:43 May 16, 2008 on arrival at Cambridge. The specific features of the distributions can be related to their locations on the map in Fig. 1 via numbers that represent the sampling points in both figures.

To evaluate the applicability of the earlier instrument calibration, the  $CF$  underway transect measurements,  $CF_U$  (the subscript “U” here and below denotes the underway data), were converted into  $CC$  units (dark green line in Fig. 2). The conversion equation  $CC = 4.40CF_U$  was derived from the correlation ( $R^2 = 0.93$ ) between  $CC$  retrievals with high performance liquid chromatography (HPLC) and the ALF  $CF$  measurements of the dark-adapted water samples representing diverse coastal and estuarine waters (Fig. 7A in [12]). As evident from comparison with the HPLC  $CC$  measurements in water samples collected along the transect (black squares in Fig. 2), the ALF  $CC$  assessments based on the nighttime or low-light measurements were in good agreement with the respective HPLC measurements

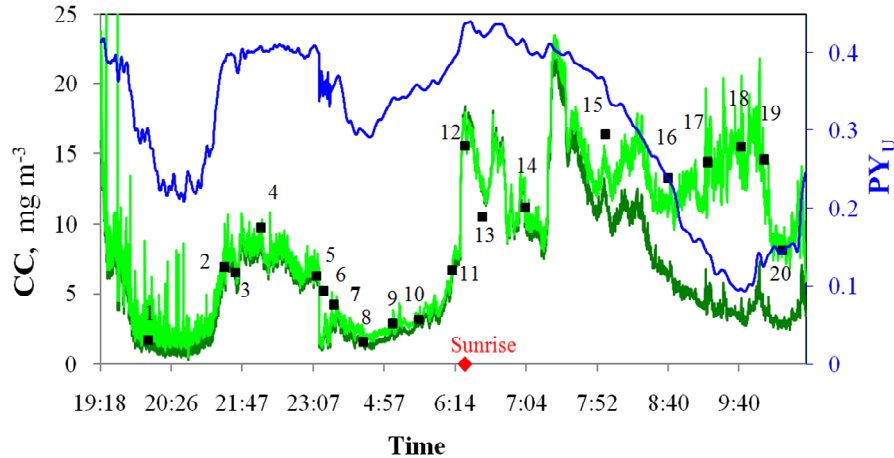


Fig. 2. HPLC measurements of Chl concentration ( $CC$ ) (black squares) and ALF underway fluorescence  $CC$  retrievals along the transect displayed in Fig. 1. *Dark green*:  $CC$  distribution calculated from the underway Chl fluorescence measurements ( $CF_U$ ) as  $CC = 4.40CF_U$  using earlier ALF calibration with dark-adapted samples. *Blue*: ALF underway measurements of PSII photochemical yield ( $PY_U$ ). *Light green*:  $CC$  distribution calculated as  $CC = 1.88CF_U/PY_U$  using correlation in Fig. 5C.

(samples 1–14). On the other hand, the morning ALF fluorescence assessments showed significant, up to 5-fold,  $CC$  underestimation of the HPLC  $CC$  measurements.

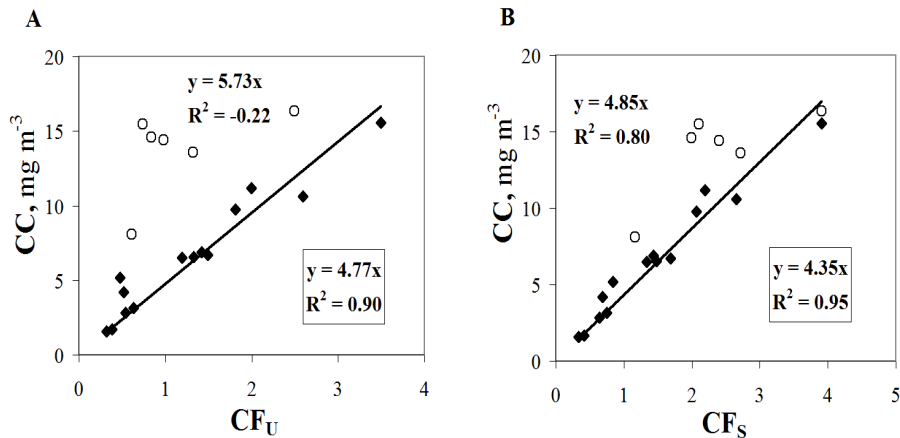


Fig. 3. Correlation between the HPLC measurements of Chl concentration ( $CC$ ) in water samples 1–20 (Figs. 1, 2) and (A) underway Chl fluorescence measurements at the sampling locations ( $CF_U$ ) or (B)  $CF$  measurements in the dark-adapted water samples ( $CF_S$ ). Diamonds and circles represent the data from the nighttime and morning portions of the transect, respectively (marked as 1–14 and 15–20 in Figs. 1, 2). The framed and unframed regression equations are calculated for nighttime and entire data sets, respectively.

Accordingly, the nighttime ALF  $CF_U$  transect measurements at sampling locations 1–14 showed high correlation ( $R^2 = 0.90$ ) with the HPLC  $CC$  retrievals for the respective samples (diamonds in Fig. 3A), and the  $CC/CF$  ratio at these locations was close to the magnitude shown by the earlier ALF calibration for the dark-adapted samples (4.77 vs. 4.40). The morning ALF transect measurements at sampling locations 15–20 showed up to 5-fold lower and variable  $CF_U$  per unit of  $CC$  (circles in Fig. 3A). That resulted in poor  $CF_U$  vs.  $CC$  correlation for the entire data set that included both the nighttime and morning measurements

( $R^2 = -0.22$ ). Similarly, the laboratory  $CF$  measurements in samples 1–14 from the low-light or nighttime of the transect showed high correlation with the HPLC  $CC$  retrievals (diamonds in Fig. 3B). The  $CC/CF$  ratio 4.35 for these samples was very close to 4.40 from the earlier ALF calibration [12], which was based on analysis of the dark-adapted samples. The morning samples 15–20 showed 10–30% lower and variable  $CF_U$  per unit of  $CC$  (circles in Fig. 3B) that resulted in lower overall  $CF_U$  vs.  $CC$  correlation ( $R^2 = 0.80$ ).

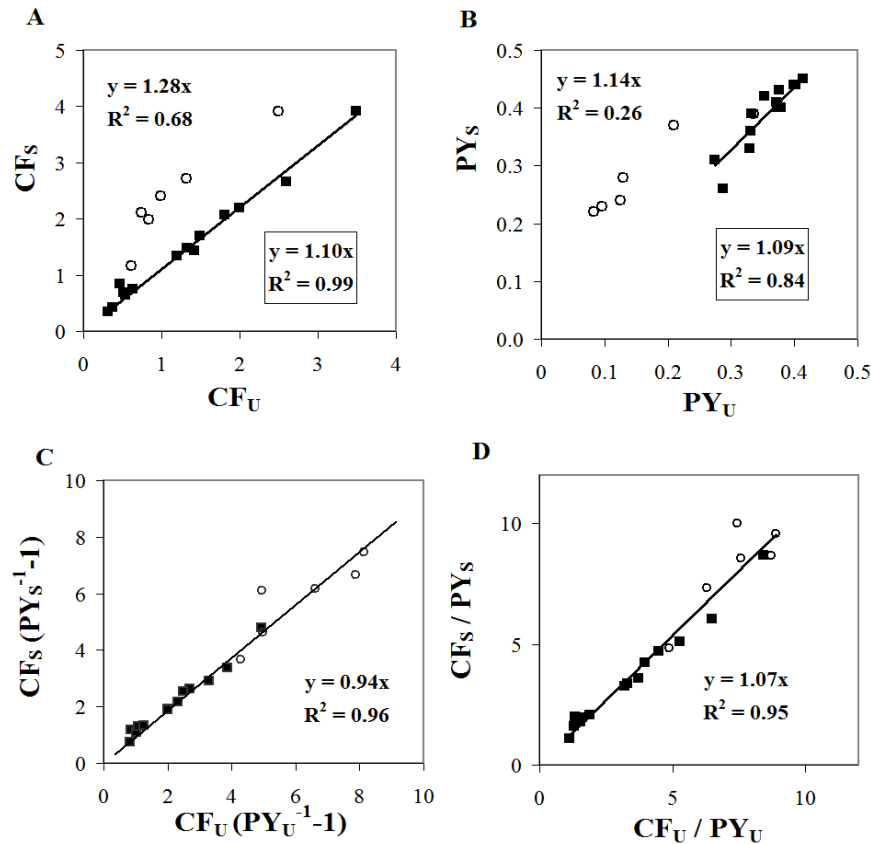


Fig. 4. (A): Comparison of Chl fluorescence in the dark-adapted water samples ( $CF_S$ ) and underway measurements at the sampling locations ( $CF_U$ ). (B): Comparison of PSII photochemical yield measured in the dark-adapted water samples ( $PY_S$ ) and underway at the sampling locations ( $PY_U$ ). Diamonds and circles represent the nighttime (samples 1–14 in Figs. 1 and 2) and morning (samples 15–20) parts of the transect, respectively. (C) and D: Comparison of fluorescence parameters  $CF(PY^{-1}-1)$  and  $CF_U/PY_U$  for the data sets displayed in panels (A) and (B).

Figures 4A and 4B allow direct comparison of the  $CF_S$  and  $PY_S$  magnitudes (the subscript “S” here and below denotes the sample measurements) measured in the dark-adapted samples and the respective underway  $CF_U$  and  $PY_U$  measurements at the sampling locations. Consistent with the plots in Fig. 3, the nighttime portion of the data (samples 1–14) show high correlation between the underway and sample measurements ( $R^2 = 0.99$  and  $0.84$  for  $CF$  and  $PY$ , respectively). The morning underway  $CF_U$  and  $PY_U$  magnitudes were noticeably lower than the respective  $CF_S$  and  $PY_S$  values, which resulted in the reduced overall correlations for the entire set of samples 1–20 ( $0.68$  and  $0.26$  for  $CF$  and  $PY$ , respectively).

Assuming that the differences between the nighttime and morning portions of the data displayed in Figs. 2, 3, 4A and 4B were caused by the  $NPQ$  of  $CF$  and  $PY$  in the sampled subsurface water in the morning hours, the  $NPQ$  invariance of the fluorescence parameters in

Eqs. (19) and (20) can be evaluated. The  $CF(PY^{-1}-1)$  magnitudes showed excellent correlation ( $R^2 = 0.96$ ) for the entire data set that includes both nighttime and morning samples 1–20 and the respective underway measurements at the sampling locations (Fig. 4C). Similarly high correlation ( $R^2 = 0.95$ ) was observed for the  $CF/PY$  parameter (Fig. 4D).

As evident from Figs. 5A and 5B, the  $CF(PY^{-1}-1)$  magnitudes showed reasonably good correlation with the HPLC  $CC$  retrievals for both the underway and sample measurements ( $R^2 = 0.74$  and  $0.83$ , respectively). The  $CF/PY$  parameter showed noticeably better correlations with the HPLC  $CC$  retrievals for both the underway and sample measurements ( $R^2 = 0.93$  and  $0.96$ , respectively, Figs. 5C and 5D). For evaluation, the  $CC_{CF/PY}$  transect distribution (light green line in Fig. 2) was calculated using the ALF underway transect measurements of  $CF_U$  and  $PY_U$ , and the regression equation  $CC = 1.88CF_U / PY_U$  from Fig. 5C.

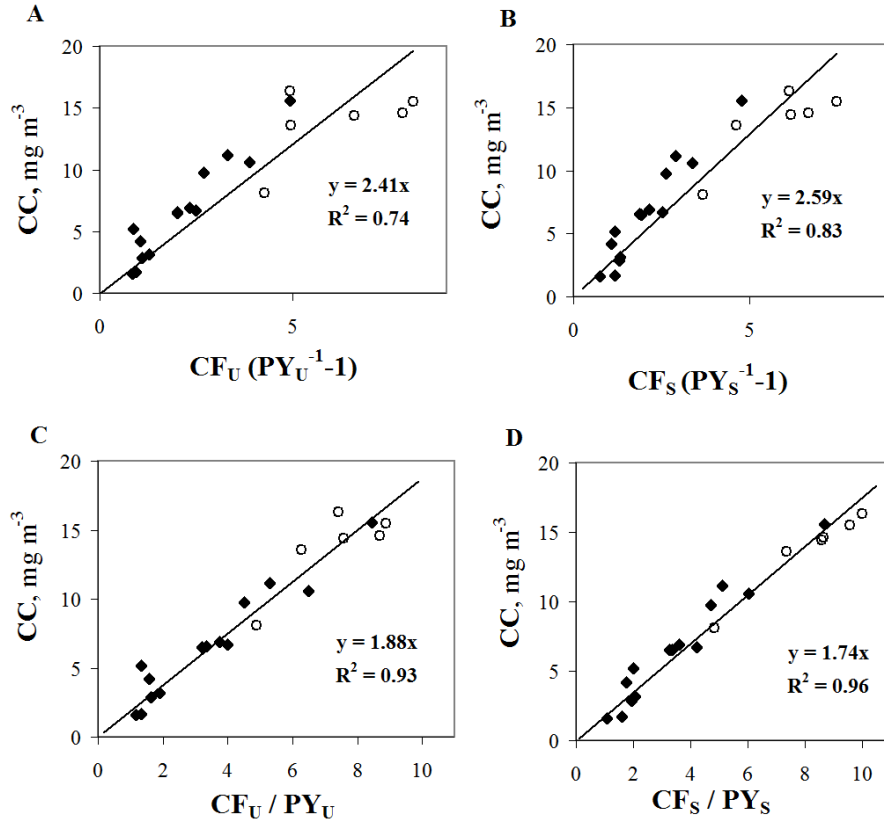


Fig. 5. (A): Correlations between the HPLC measurements of  $CC$  in water samples and fluorescence parameters  $CF(PY^{-1}-1)$  and  $CF/PY$  calculated from Chl fluorescence ( $CF$ ) and PSII photochemical yield ( $PY$ ) measured in the dark-adapted water samples (B) and (D) and the underway flow-through  $CF$  and  $PY$  measurements at the sampling locations (A) and (B) marked as 1–20 in Figs. 1 and 2. Diamonds and circles represent the nighttime (samples 1–14) and morning (samples 15–20) parts of the transect, respectively.

## 6. Discussion

### 6.1. Practical implementation of the four-step protocol

A four-step measurement protocol is proposed in section 3 to reduce the  $PQ$  and  $NPQ$  effects on the  $CF$  retrievals. The ALF *in vivo*  $CF$  measurements using this protocol show high correlation with independent HPLC  $CC$  retrievals (for example, see diamonds in Fig. 3A and 3B; see also Fig. 7A in [12]). Recent ALF field deployments have confirmed that *in vivo*  $CF$

measurements compliant with the four-step protocol can indeed provide high-accuracy *CC* assessments. In coastal and estuarine waters that are typically dominated by diatoms and dinoflagellates, the relationship between *CF* and *CC* can be described by a simple regression equation (e.g.,  $CC = 4.40CF$  for the ALF measurements [12]) that does not show significant seasonal or regional variability. A more complex, non-linear relationship may need to be used in the offshore oceanic waters, particularly in the frontal zones that exhibit strong gradients in physical and chemical properties [50].

Some aspects of the practical implementation of the four-step protocol are briefly discussed below. Many benchtop and some *in situ* fluorometers are equipped with a dark measurement chamber that provides optical isolation of the phytoplankton-containing water volume (condition # 1 of the protocol). Technically, the PSII saturating excitation (condition # 2) can be provided by selecting an appropriate light source for fluorescence excitation and through instrument design. For example, 405 and 532 nm lasers are used for this purpose in the ALF instrument. The small cross-section and low divergence of the laser beam simplifies optimization of the optical design. The narrow-bandwidth laser excitation minimizes the spectral bandwidth of the water Raman scattering and allows for spectral deconvolution of the overlapped fluorescence bands of seawater constituents [12]. Light emitting diodes used for fluorescence excitation in various instruments, including PSII saturating fluorometers for measuring variable fluorescence, can provide a cost-efficient alternative to lasers.

Some relevant aspects of optimizing sample exposure to the excitation light (condition # 3) can be illustrated using the field data presented in Results. While both nighttime underway *CF* measurements and analyses of nighttime water samples showed high correlation with *CC* ( $R^2 = 0.90$  and  $0.95$ , respectively in Fig. 3A, B), the slopes in the correlation equations were noticeably (~10%) different. The regression equation in Fig. 4A also suggests that the underway measurements yielded 10% lower *CF* magnitudes than the sample measurements. As discussed in section 4, this difference can be explained by shorter exposure of phytoplankton to the excitation due to the 10-fold faster flow rate used for the underway measurements. Much stronger *CF* dependence on the sampling flow rate can be observed under less intense fluorescence excitation intensity used in many instruments (e.g., [48]).

Generally, the sample exposure time needs to be optimized to reduce the *CF* dependence on the measurement protocol. For *CF* measurements at the MT PSII turnover scale using PSII saturating excitation, it can be optimized with regard to the Kautsky effect [44, 47]. Under these conditions, a 1–3 second exposure may appear to be optimal. Then, after reaching  $\Phi_{m(MT)}$  during the initial 100–200 ms of Kautsky induction (see Section 4), *CFY* would remain at this level during most of the exposure time. When measuring the stationary sample, the *CF* measurements can begin when *CFY* reaches  $\Phi_{m(MT)}$  and end before beginning manifestation of excitation-induced *NPQ*, which develops after ~3 seconds under such conditions (Fig. 1 in [47]). The signal integration time can be adjusted in some range (assuming *CFY* is still  $\sim\Phi_{m(MT)}$  during the measurement) to optimize the measurement protocol. In the case of flow-through measurements, the signal integration time can be longer than the exposure time to ensure the desirable signal-to-noise ratio.

In practice, the need for prolonged (~1 hour) phytoplankton dark adaptation before the fluorescence measurements (condition # 4) limits the four-step protocol mainly to laboratory use (including shipboard measurements). For field *CF* measurements in stationary settings (e.g. moorings, piers, etc.), the instrument can be equipped with a sampling chamber to provide adequate dark adaptation prior to the measurements. It should be noted that, based on our field experience, even several hours of dark adaptation is often insufficient for complete recovery from the photoinhibitory *NPQ* [39, 44] developed in the PSII RCs in subsurface water exposed to excessive solar irradiance. For example, the “leftover” *NPQ* effect was evident in *CF* measurements of the morning surface samples discussed in Results. After 2–3 hours of dark adaptation, these samples showed an increase in *CF/CC* magnitudes vs. the real-time underway measurements, which were strongly affected by *NPQ* (circles in Figs. 3B

and 3A, respectively), but these values were still variable and lower than the night-collected samples (diamonds in Fig. 3B). Only one morning sample (# 15 in Fig. 2) that had the smallest exposure to solar irradiance after sunrise and the longest (~4 hour) duration of dark adaptation, showed complete recovery from *NPQ*. This is indicated by the fact that the *CF/CC* ratio is identical to the night-collected samples ( $CF_S = 4$  in Fig. 3B). Note that the same underway and sample data showed no difference between the morning and night measurements when the *NPQ*-invariant fluorescence parameter was used to correlate with *CC* (Figs. 5C and 5D).

## 6.2. *CF* adjusting for *NPQ* using *PY* measurements

In the case of continuous underway or *in situ* measurements, it is practically impossible to provide dark adaptation long enough to eliminate *NPQ* caused by phytoplankton exposure to ambient light prior to measurement. This may result in significant uncertainty in *CC* fluorescence assessments using instrument calibration with dark-adapted phytoplankton (for example, see Fig. 2). Even with an adequate analytical model, it is difficult to estimate the *NPQ* magnitude that is determined by the usually unknown phytoplankton light history. The above analysis shows that it may be possible to adjust the *NPQ*-affected *CF* measurements using concurrent measurements of variable fluorescence that yield *PY* magnitudes. The field data in Results allows for evaluating the feasibility of *CC* assessment using the *NPQ*-invariant fluorescent parameters derived from *CF* and *PY* measurements. In particular, the data sets used for calculation of  $CF(PY^{-1}-1)$  and  $CF/PY$  data in Figs. 4C and 4D included both *NPQ*-free and *NPQ*-affected data from sampling locations 1–14 and 15–20, respectively (Fig. 2). Despite significant variability in the *NPQ* magnitudes (Figs. 3, 4A, 4B), both  $CF(PY^{-1}-1)$  and  $CF/PY$  variables showed strong correlation ( $R^2 = 0.96$  vs.  $0.95$ , respectively, in Figs. 4C and 4D), thus demonstrating their *NPQ* invariance.

It should be noted that both *CF* and *PY* were measured using PSII saturating excitation. Under this condition for the dark-adapted phytoplankton,  $PY = \Phi_p^m$  [12] and *CF* is proportional to  $\Phi_m$  (see Section 4); the same is valid for light-adapted phytoplankton with the respective change in notation,  $\Phi_p'^m$  and  $\Phi_m'$ . Thus, the *NPQ* invariance of  $CF(PY^{-1}-1)$  (Fig. 4C) is fully consistent with the above model analysis (see Eq. (20)). On the other hand, despite the similarity between  $CF/PY$  and  $\Phi_f/\Phi_p$  ratios, the PSII saturating excitation is not described by Eq. (19), which actually predicts *NPQ*-invariance of  $\Phi_f/\Phi_p$ . Therefore, the experimentally observed *NPQ* invariance of the  $CF/PY$  parameter (Fig. 4D) is not justified by the simplified biophysical model discussed in Section 2. Nonetheless, this observation is still reported here, as it may provide new insight for better understanding of phytoplankton photosynthetic regulation in natural conditions and assist in improving *CC* fluorescence assessments.

Though both parameters performed equally well in terms of *NPQ*-invariance (Figs. 4C and 4D), the  $CF/PY$  ratio for both underway and sample retrievals showed better correlation with the HPLC *CC* measurements ( $R^2 = 0.93$  and  $0.96$ , respectively; Fig. 5). The  $CF(PY^{-1}-1)$  parameter calculated from the underway measurements at sampling locations 1–20 also showed a dramatic improvement in correlation with the HPLC *CC* data as compared to the *CF* magnitudes for the same data set ( $R^2 = 0.74$  vs.  $-0.22$  in Figs. 5A and 3A, respectively).

Thus, the  $CF(PY^{-1}-1)$  parameter can be used for reasonably accurate *CC* assessments from *NPQ*-affected measurements of *CF* and *PY*. A potential downside is that this parameter may appear to be more sensitive than *CF* to potential variability in the PSII photochemical functionality (determined by *f* in our model). Indeed, according to the model,  $CF(PY^{-1}-1) \sim F_o/F_p^m = k_f/fk_p$ , while *CF* does not depend on *f* due to the PSII-saturating excitation. In particular, the significant transect variability in  $PY_U$  (and, respectively, *f* (see Eq. (6))) evident in the Fig. 2 might account for  $CF(PY^{-1}-1)$  correlation with HPLC *CC* that

was lower than for nighttime,  $f$ -independent underway  $CF$  measurements (0.74 vs. 0.90 in Figs. 5A and 3A, respectively).

This may also explain the only marginal improvement in the  $CF(PY^{-1}-1)$  correlation with HPLC  $CC$  as compared to the  $CF$  correlation for the dark-adapted samples ( $R^2 = 0.83$  vs.  $0.80$  in Figs. 5B and 3B, respectively). If our interpretation is correct, the  $PQ$  variability in  $CF$  was minimized by using PSII saturating excitation, but the  $CF$  magnitudes in the morning samples were still moderately  $NPQ$ -affected because of their incomplete recovery from  $NPQ$  (empty dots in Fig. 3B). This “leftover”  $NPQ$  effect was not manifested in the  $CF(PY^{-1}-1)$  parameter, but the overall transect variability in the PSII photochemical functionality might have affected the  $CF(PY^{-1}-1)/CC$  relationship.

Similar comparisons for the  $CF/PY$  parameter revealed significant improvements in correlations with HPLC  $CC$  retrievals for both the underway and sample measurements:  $R^2 = 0.93$  vs.  $-0.22$  in Figs. 5C and 3A;  $R^2 = 0.96$  vs.  $0.80$  in Figs. 5D and 3B. Though the use of  $CF/PY$  parameter was not justified by the simplified biophysical model and needs further consideration, the  $CF/PY$  ratio may be advantageous vs. the  $CF(PY^{-1}-1)$  parameter for minimizing the effects of both  $NPQ$  and  $PQ$  variability on the accuracy of  $CC$  fluorescence assessments. For evaluation, the linear regression relationship  $CC = 1.88CF_U/PY_U$  between  $CC$  and underway fluorescence measurements at the sampling locations (Fig. 5C) was used to calculate the  $CC$  transect distribution (light green line Fig. 2). As evident from comparison with the independent  $CC$  sample measurements, the concurrent  $CF$  and  $PY$  measurements provided accurate high-resolution  $CC$  data despite the significant  $NPQ$  and PSII physiological variability in the water masses.

## 7. Conclusion

The biophysical analysis and field measurements show that significant (up to 15-fold) photo-physiological variability in fluorescence yield is one of the major factors contributing to the overall variability in *in vivo* chlorophyll fluorescence per unit of chlorophyll concentration. The fluorescence yield and PSII photochemical efficiency are controlled by  $PQ$  and  $NPQ$  mechanisms and depend on incident light intensity, phytoplankton “light history”, PSII photochemical functionality, and other physiological factors. Minimizing the  $PQ$  and  $NPQ$  magnitudes can help to reduce the variability and improve the accuracy of  $CC$  fluorescence assessments. This can be achieved via isolation of the measurement volume from ambient light, PSII saturating fluorescence excitation, optimization of phytoplankton exposure to the excitation, and phytoplankton dark adaptation before the measurements. If the measurement conditions do not allow for dark adaptation (e.g., *in situ* or flow-through underway measurements from a moving platform), concurrent measurements of variable fluorescence can be used to adjust fluorescence intensity for non-photochemical quenching developed due to prior exposure to ambient light. The field evaluation in estuarine waters of the Chesapeake and Delaware Bays showed significant potential of this approach for improved fluorescence assessments of chlorophyll concentration. Nonetheless, it needs evaluation in more diverse coastal and offshore oceanic waters. An improved biophysical model needs to be developed to account for the complexity of the photo-physiological mechanisms involved.